# Using Satellite Images for Drought Monitoring: A Knowledge Discovery Approach

**Getachew Berhan**
**Addis Ababa University, Ethiopia**

**Shawndra Hill**
**University of Pennsylvania**

**Tsegaye Tadesse**
**University of Nebraska-Lincoln**

**Solomon Atnafu**
**Addis Ababa University, Ethiopia**

*The main objective of this research was to develop a new concept and approach to extract knowledge from satellite imageries for near real-time drought monitoring. The near real-time data downloaded from the Atlantic Bird satellite were used to produce the drought spatial distribution. Our results showed that approximately 40% of the observed areas exhibited negative deviation. In this study, the possibility of using the near real-time spatio-temporal Meteosat Second Generation (MSG) data for drought monitoring in food insecure areas of Ethiopia was tested, and promising results were obtained. The output of this research is expected to assist decision makers in taking timely and appropriate action in order to save millions of lives in drought-affected areas.*

## INTRODUCTION

Because of climate change and variability, drought has become a recurrent phenomenon in several countries across the globe. It is manifested in erratic and uncertain rainfall distribution in rainfall-dependent farming areas, especially in arid and semi-arid ecosystems. Frequent and severe drought has become one of the most important natural disasters in sub-Saharan Africa and often results in serious economic, social, and environmental crises (Tadesse et al., 2008) marked by the creation of uncertain agricultural economies (Kandji &Verchot 2006).

Ethiopia is a sub-Saharan country that has been affected by drought. Millions of lives have been lost because of recurring droughts in the past several decades (Ibid). Due to climatic changes, drought occurs every two years in different parts of Ethiopia (Kandji &Verchot 2006; NMSA, 1996). In addition, the drought recurrence cycle shortens over time while the affected area is widening, impacting additional parts of the country that were once unaffected (NMSA, 1996). In order to respond to the effects of drought, Ethiopia has been conducting drought assessment and monitoring missions.

In Ethiopia, drought assessment and monitoring efforts have been based on conventional methods that rely on the availability of meteorological data, which is very tedious and time consuming to collect. Moreover, meteorological data and weather information dissemination is also a challenge. Consequently, millions of lives may be lost before the actual information is submitted to the appropriate decisions makers (Kandji &Verchot 2006). The information that is produced in accordance with the conventional approach is usually highly uncertain for employing rescue missions; therefore, producing reliable and timely information for decision makers is of the utmost importance.

Traditionally, there are several operational indices in drought assessment and monitoring that are based on rainfall data. These indices are often not easily accessible, nor are they tailored to be conveniently understood by decision makers (Ji & Peters, 2003). The common approach that is used to derive the necessary information is the application of climatic drought indices, such as the Palmer Drought Monitoring Index, which has been widely used by the U.S. Department of Agriculture (Jain et al., 2009). Another popular climatic drought index is the Standardized Precipitation Index (SPI) that was developed by McKee et al. (1993), which can identify data on emerging drought months for regional and global applications. Mishra and Desai (2005) have adopted the SPI for parts of India and have used that data to compile a drought severity area frequency curve. These drought severity and monitoring indices are based on point data that are measured at the different meteorological stations located in a wide area. In remote areas where there is not a dense network of stations, extrapolation of rainfall observation from nearby stations is commonly used, resulting in high uncertainty about its usefulness for real-time rescue missions.

At the present, decision makers in many countries use remote sensing to close this gap and obtain the desired information. Remote sensing data, or data from satellite sensors, can provide continuous datasets that can be used to detect the onset of a drought as well as its duration and magnitude (Thiruvengadachari & Gopalkrishana, 1993). Remote sensing is far superior to conventional methods (Jain et al., 2009) for drought monitoring and early warning applications. The challenge in applying remote sensing data in drought monitoring and in issuing early warnings is that the various indices must be validated and calibrated to the specific region and ecological conditions (Singh et al., 2003; Jain et al., 2009). So far, no significant efforts have been made to validate and calibrate remote sensing data in food insecure areas within Ethiopia. Thus, the available information is unclear, uncertain, and difficult for decision makers to access (FEWS NET, 2009). In addition, even though drought has its own state and behavior, there have been no past efforts to detect drought by its own properties as a spatial object (Rulinda et al., 2010).

In remotely sensed images, a pixel or group of pixels with similar spectral reflectance characterize the object of interest. Remote sensing object classification methods usually consider texture information of features on the earth. Pixels identified as having the same texture are grouped together, and those groups are considered objects (Benz et al., 2004), which can represent physical features on earth, such as roads, parcels, or bodies of water. When these physical features are classified based on texture, they are considered to be physical objects (Ibid).

The concept of object identification and analysis can be extended to non-physical features on the ground, and are usually referred to as virtual geographic objects (Batty et al., 1999), which can be defined as measurements having geographic information but not representing physical features on earth (Huang et al., 2001). The objects in this case are defined based on some attributes of their physical features. Drought is a virtual geographic object, and in this research, we used NDVI and NDVI deviation values of satellite images to characterize its incidence. In the actual identification and analysis of drought in this research, the concept of virtual GIS techniques was used. Virtual GIS uses the "knowledge base" that is inherent in GIS for automatic interpretation of remotely sensed images (Batty et al., 199). This is based on the principles of virtual geography, which is the study of place as ethereal space and its process inside computers, and the ways in which this space inside computers is changing material place outside computers (Ibid).

The concept of virtual reality is very important in the identification and representation of drought objects on the real ground and in computer representation. Virtual reality is a computer graphic technology that can be used to emulate the real world in different dimensions, with which users can participate in the virtual environment by applying different data manipulation mechanisms (Huang et al., 2001)

The main objective of this research was to develop a new concept and approach to extract knowledge from satellite imageries for near real-time drought monitoring. Advanced technology satellite products with high temporal resolution (e.g., MSG data every 15 minutes) are cost effective and can serve to detect the onset of a drought and its duration and magnitude. Such information can help decision makers to take appropriate actions in a timely manner, reduce the impact of drought conditions, and mitigate drought's adverse effects on the environment. This effort is indicated to be one of the climatic change mitigation efforts for countries that have been affected by recurrent droughts in the past (Kandji &Verchot 2006).

## AN OVERVIEW OF DROUGHT MONITORING AND MODELING

Drought is defined as "the naturally occurring phenomenon that exists when precipitation has been significantly below normal recorded levels, causing serious hydrological imbalances that adversely affects land resource production systems" (UNCCD, 1999). Drought is also defined as a prolonged abnormally dry period when there is not enough water for users' normal needs, resulting in extensive damage to crops and a loss of yields (Wilhite, 2005). These definitions are conceptual explanations that provide the basis for the operational meaning. The operational definition of drought focuses on identifying the beginning, end, spatial extent, and severity of the drought in a given region and is based on scientific reasoning. The analysis is conducted by using hydro-meteorological information and is beneficial in developing drought policies, early warning monitoring systems, mitigation strategies, and preparedness plans (Smakhtin & Hughes, 2004). Generally, the most prominent types of drought are meteorological, agricultural, and hydrological droughts (Wilhite, 2000; Obasi, 1994) (Figure 1a). Meteorological drought is usually defined according to the degree of dryness (i.e., in comparison to the "normal" or average amount of precipitation of the region) and the duration of the dry period at a particular place and at a particular time. Hydrological drought is associated with the effects of periods of precipitation (including snowfall) shortfalls on the surface or subsurface water supply (i.e., stream flow, reservoir and lake levels, and ground water). Although all droughts originate from a deficiency of precipitation, hydrologists are more concerned with how this deficiency plays out through the hydrologic system. Hydrological drought is associated with the effects of low rainfall on the water levels of rivers, reservoirs, lakes and aquifers. Agricultural drought links various characteristics of meteorological and hydrological drought to agricultural impacts, focusing on precipitation shortages, differences between actual and potential evapo-transpiration, soil water deficits, and reduced ground water or reservoir levels (Wilhite, 2000). Agricultural drought occurs when there is not enough water available for a particular crop to grow at a particular time. This research focuses on agricultural drought analysis and an early warning system. The frequency of agricultural drought in Ethiopia is presented in Figure 1b and c.

The process of monitoring agricultural (i.e., vegetative) drought usually requires remote sensing technologies and a large amount of temporal data, in addition to traditional climate information. The most widely used source of satellite data is the NDVI (Rulinda et al., 2010), which is commonly calculated by using image data from polar orbiting satellites that carry sensors that detect radiation in red and infrared wavelengths (Fensholt et al., 2006). The NDVI is used, in this case, by comparing the deviation of the current satellite observation from the historical average within a certain time period, or window, of interest. In the analysis of droughts, their onset, duration, and severity are often difficult to determine and the characteristics may vary significantly from one region to another (Rulinda et al., 2010). In rainfall-dependent agriculture production areas, seasonal rainfall variability is inevitably reflected in both highly variable production levels and in the risk-averse livelihoods of local farmers (Cooper et al., 2008). Africa has a long history of rainfall fluctuations of varying lengths and intensities (Nicholson, 1994), primarily because of climate changes. Recent studies indicate varying behavior of rainfall trends in Africa at different spatial and temporal scales. A recent study also demonstrated a decrease in rainfall in east Africa between 2003 and 2008 (Swenson & Wahr, 2009), in which drought and famine situations were periodically reported (FEWS NET, 2009). Drought has a particularly negative impact on agricultural production in the eastern African region because most of the agriculture there is dependent on rainfall rather than irrigation (Thorton et al., 2009).

The conventional approach to drought monitoring and early warning systems that uses ground-based data collection is tedious, time consuming, and difficult (Prasad et al., 2007). In recent years, remote sensing data has been used to monitor agro-climatic conditions, the state of the agricultural fields, vegetation cover, and to estimate crop yield in various countries. In particular, the Advanced Very High Resolution Radiometer (AVHRR) NDVI information has been used in vegetation monitoring, crop yields assessment, and forecasting (Hayes et al., 1982; Benedetti & Rossini, 1993; Quarmby et al., 1993; Unganai & Kogan, 1998; Kogan et al., 2003). The National Oceanic and Atmospheric Administration's (NOAA) AVHRR series satellite feedback provides a long-term record of NDVI data that can be used to predict crop yield (Prasad et al., 2007). Yield prediction is part of the drought monitoring process in that crop yield information is essential to determine the food assurance of a given region.

**Drought Object Modeling**

The concept of object identification and modeling has been an ongoing scientific effort for converting remotely sensed images into geographic phenomena (Stein et al., 2009). In this research, an object is noted in the context of object-oriented modeling (Woryboys et al., 1990); this is based on the basic principle that an object has two characteristics: state and behavior (Woryboys et al., 1990; Budd, 2000). State is the attribute or information contained in an object, and behavior is the set of actions in which an object performs (Budd, 2000). When identifying and modeling the drought object by using satellite images, state refers to the actual reflectance attributes (i.e., the digital numbers that are registered by the satellite sensors as pixel values or index values, such as NDVI), and behavior means that when a drought object occurs on the ground, plants die or cease the process of photosynthesis (i.e., the red band of the spectrum is not used by the plant and is reflected back to the satellite sensor). As a consequence, yield is reduced in the long-term effects (Tucker, 1979; UNISDR, 2009).

There are two key questions to be asked when identifying the state and behavior of any object: "what possible states (i.e., attributes) can a give object be in", and "what possible behavior (i.e., actions) can this object perform when it happens?" (Budd, 2000). The geographic object that we are interested in for this research is agricultural drought – where it results in reduced biomass and yield (Wilhite, 2005).

The concept of identifying and modeling drought as an object is new (Rulinda et al., 2010). Rulinda et al. (2010) further indicate that "a next step in drought modeling is an approach focusing on spatial object and this kind of object can be built from different temporal resolution images". In remote sensing, objects are identified and subsequently classified on the basis of pixel information, and the objects are subsequently tracked in time, during which, their behavior may be governed by external factors that must also be identified and quantified (Stein et al., 2009). This process is usually accomplished through image mining techniques.

Image mining is defined as the analysis of large sets of observational images to find suspected or unsuspected relationships and to summarize the data in novel ways that are both understandable and useful to stakeholders (Stein, 2008). Object identification in remote sensing is usually conducted by converting raster pixel values to geographic objects. Usually, the image is segmented first, providing approximately homogeneous segments, then classified (Stein et al., 2009). Stein et al. (2009) further states that various procedures for image segmentation are well-documented, and include procedures based on mathematical morphology, edge detection, and the identification of homogeneity in one band or in a set of bands. Classification practices include statistical routines, such as k-nearest neighbour classifiers, and increasingly fuzzy classification methods (Ibid).

**FIGURE 1**
**DROUGHT CLASSIFICATION**
**(adapted from UNISDR 2009)**
**(a); frequency of agricultural droughts in Ethiopia during the first rainy seasons (February – May)**
**(b); and second rainy seasons (July - September)**
**(c) (adapted from NMSA, 1996)**

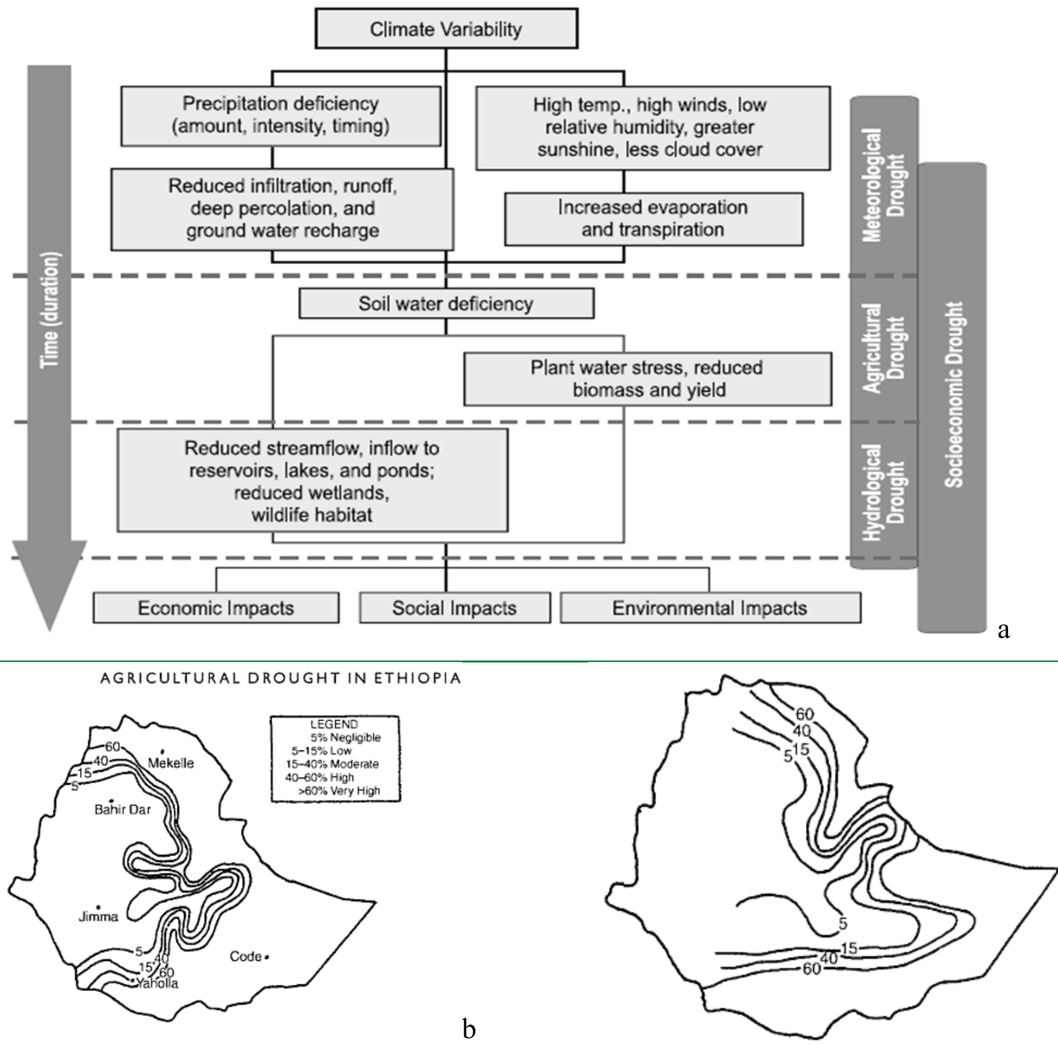


## MATERIALS AND METHODS

### Theoretical Framework

One of the criteria for innovative academic research is that it must have a clearly defined theoretical framework, which helps to differentiate research from consultants' work (Gregor, 2006). Defining the theoretical framework for a given study also helps to accumulate knowledge in a systematic manner; such knowledge enlightens professional practice (Gregor, 2006; Gregor & Jones, 2007). Taking this fact into account, the theoretical framework for this research is "design science." Gregor (2006) indicates that "design theory" provides explicit prescriptions for constructing an artifact and mainly answers the question of how to do something.

Design science is a problem-solving process. In their problem-solving process, Hevner et al. (2004) present seven guidelines with which to conduct design science research. These guidelines consider the design as an artifact, problem relevance, design evaluation, research contributions, research rigor, design as a search process, and finally, the communications of research. The study presented in this paper modifies Hevner's et al. (2004) seven guidelines into five steps: identification, modeling, tracking, prediction, and communication with stakeholders. The artifact for the process of knowledge discovery from satellite images is presented in Figure 2.

An artifact is used to describe something that is artificial or constructed by humans, as opposed to something that occurs naturally (Simon, 1996). In this research, "artifact" signifies the abstract representation of the design science research process and its final information delivery to decision makers.

**FIGURE 2**
**AN ARTIFACT FOR THE PROCESS OF KNOWLEDGE DISCOVERY FROM SATELLITE IMAGERIES**
**(adopted from Stein et al., 2009)**

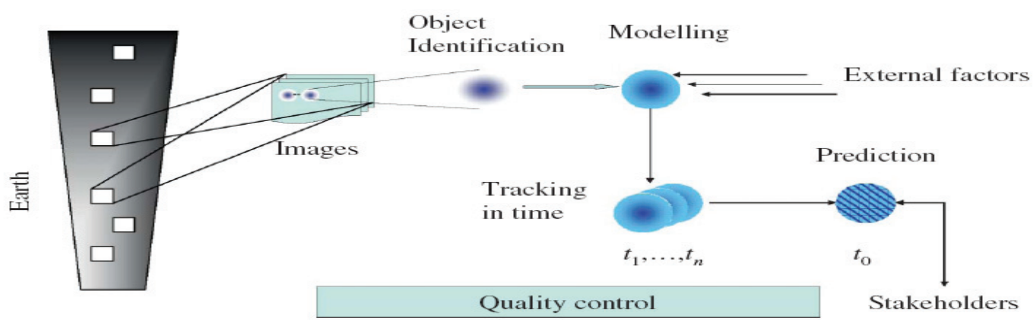


**Study Area**

The study area for this research is the whole of Ethiopia, which occupies the interior of the eastern Horn of Africa, stretching between $3^0$ and $15^0$ N latitude and $33^0$ and $48^0$ E longitude, with a total area of 1.13 million $km^2$ (EMA, 1988).

Ethiopia is located in the tropics and variations in altitude have produced a variety of microclimates. The mean annual rainfall ranges from 2,000mm in some pocket areas in the southwest highlands, to less than 250mm in the lowlands. In general, annual precipitation ranges from 800mm to 2,200mm in the highlands (>1500 meters above sea level) and varies from less than 200mm to 800mm in the lowlands (<1500 meters above sea level). Rainfall also decreases northwards and eastwards from the high rainfall pocket areas in the southwest (NMSA, 1996).

**Methods**

The satellite data were extracted using geographic information systems (GIS) techniques. ILWIS 3.6 software was used in the analysis of the remote sensing imagery. The near real-time data downloaded from the Atlantic Bird satellite, were used to produce the drought monitoring indices. During the analysis, cloud-contaminated pixels were removed from each individual image by examining the reflectance and temperatures. After completing the pre-processing of the satellite images, the NDVI values of the images were calculated using Equation 1:

$$NDVI = \frac{\rho_{nir} - \rho_{red}}{\rho_{nir} + \rho_{red}} \quad (1)$$

where $\rho_{red}$ (0.4–0.7 mm) and $\rho_{nir}$ (0.75–1.1 mm) are reflectance in red and near infrared bands of the satellite imageries, respectively.

NDVI is the most commonly used vegetation index. It has been shown to be related to vegetation vigor, percentage green cover, and biomass (Myneni & Asrar, 1994; Anyamba & Tucker, 2003; Pettorelli & Vik 2005). It is a non-linear function that varies between -1 and +1, and is undefined when both $\rho_{red}$ and $\rho_{nir}$ are zero. NDVI values for vegetated land areas generally range from approximately 0.1 to 0.7. Values greater than 0.5 indicate dense vegetation, whereas values lower than 0.1 indicate near zero vegetation such as barren area, rock, sand, or snow (Tucker, 1979).

In this research, the daily NDVI values were aggregated into a decadal basis from MSG satellite data. In one year, there are 36 dekads (one dekad is equal to 10 days). The decadal NDVI values were compared with the long-term mean NDVI value of the same dekad from NOAA AVHRR satellite data. The difference between these two data elements is called deviation of drought severity index, or the deviation of the NDVI (Dev_NDVI) (Tucker, 1979). The Dev_NDVI was calculated using Equation 2. When the Dev_NDVI is negative, it indicates below normal vegetation conditions and might suggest a drought situation (Tucker, 1979). We used Dev_NDVI to spatially locate the occurrence of drought.

$$Dev\_NDVI = NDVI\_i - NDVI\_Mean\_i \qquad (2)$$

where $NDVI\_i$ and $NDVI\_Mean\_i$ are the actual 10-day composite NDVI and the long-term mean for the same dekad NDVI values, respectively. $NDVI\_i$ was acquired from MSG and $NDVI\_Mean\_i$ from NOAA.

**Materials**

For this study, satellite data from Meteosat Second Generation (MSG) and National Oceanic and Atmospheric Administration (NOAA) AVHRR were used. MSG is the new European system of geostationary meteorological satellites with the associated infrastructure; it was developed to succeed the highly successful series of original Meteosat satellites that has served the meteorological community since the first launch in 1977 (EUMETSAT, 2005). The advanced Spinning Enhanced Visible and Infrared Imager (SEVIRI) radiometer onboard the MSG satellites enables the Earth to be scanned in 12 spectral channels from visible to thermal infrared at 15 minute intervals. Each of the 12 channels has one or more specific applications, either when used alone or in conjunction with data from other channels. From these 12 channels, this research used Channels 1 and 2 to detect vegetation condition. These two visible channels are well known from similar channels of the AVHRR instrument flown on NOAA satellites and can be used in combination to generate vegetation indices, such as NDVI (EUMETSAT, 2005).

NOAA is owned by the U.S. government; the sensor on board NOAA mission that is relevant for earth observation is a very high-resolution radiometer (AVHRR). NOAA and NASA have jointly produced long-term AVHRR datasets that have been consistently processed for global change research. These datasets cover the period from July 1981 to present and are 10-day composites of daily data [red, near infrared (NIR), and thermal wavelengths] that are mapped to a global equal area projection (EUMETSAT, 2005). There are three 10-day composites per month; the first is for days 1 through 10, the second is for days 11 through 20, and the third is for the remaining days. The data contains NDVI, a highly correlated parameter to surface vegetation, derived from the visible and NIR channel reflectance (EUMETSAT, 2005; Holben, 1986). This pathfinder dataset has gone through many stages of calibration and correction (Smith et al., 1997).

## RESULTS AND DISCUSSIONS

### Relationships Between Precipitation and NDVI

In order to analyze the relationship between RF and NDVI values, data collected from 1982 through 2004 were used. These years were selected because there were complete data sets for both RF and imageries during those time periods. The RF data was obtained from the National Meteorological Agency of Ethiopia and the NDVI values were taken from http://earlywarning.cr.usgs.gov/adds/datathemephp.

To observe the relationships between RF and NDVI, Ethiopia was divided into 22 grids; each grid was 2 degrees by 2 degrees (Figure 3). From 1982 to 2004, the RF recorded by all stations inside the grids was averaged and an average point data was generated. The same procedure was followed for the NOAA AVHRR NDVI values of the 2 degrees by 2 degrees grids. The descriptive statistics for the 6-month average values for both RF and NDVI are presented in Table 1. In addition, the scatter plots for the 4-month period average values from June to September are presented in Figure 4.

**FIGURE 3**
**THE MAP OF ETHIOPIA WITH 2x2 DEGREE GRIDS**

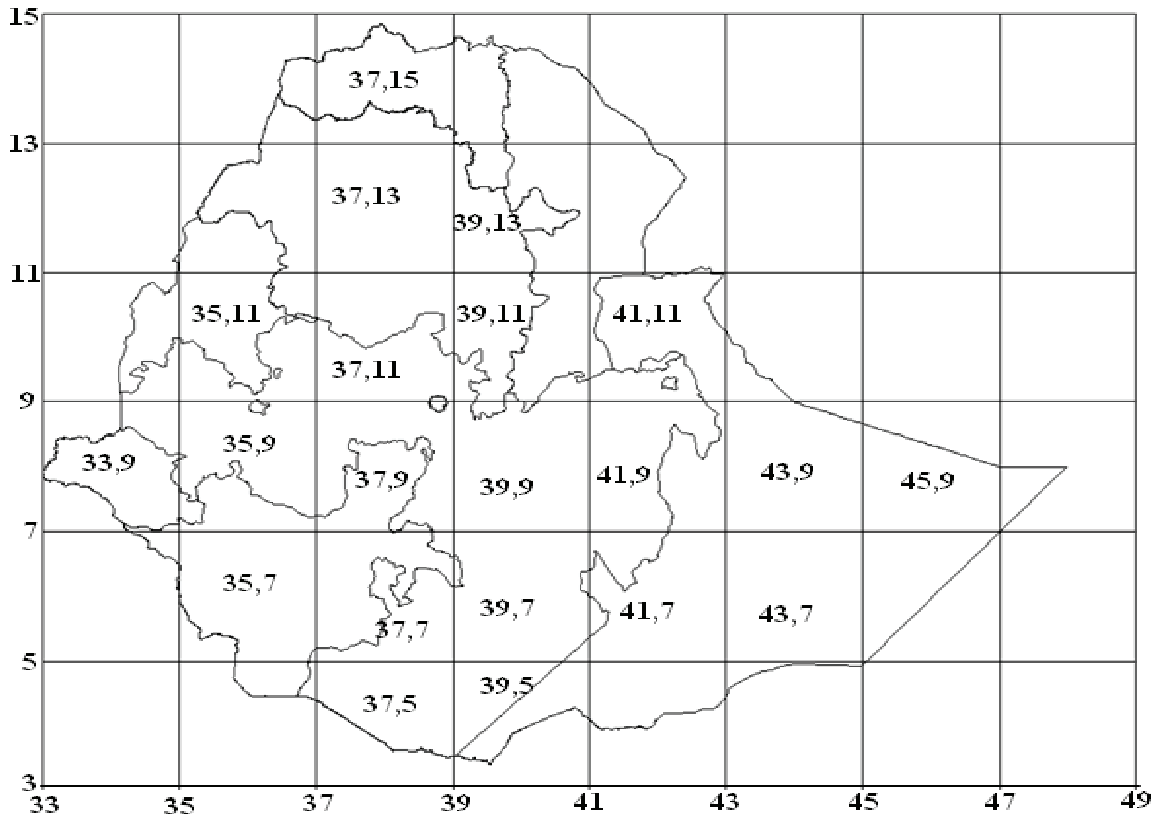

**TABLE 1**
**DESCRIPTIVE STATISTICS FOR AVERAGE NDVI AND AVERAGE RF FROM 1982-2004**

| Items | June | | July | | August | | September | |
|---|---|---|---|---|---|---|---|---|
| | *NDVI* | *RF* | *NDVI* | *RF* | *NDVI* | *RF* | *NDVI* | *RF* |
| Mean | 0.35 | 84.73 | 0.33 | 141.97 | 0.36 | 147.03 | 0.39 | 104.35 |
| Median | 0.30 | 51.90 | 0.31 | 128.67 | 0.36 | 148.26 | 0.39 | 98.83 |
| Standard Deviation | 0.14 | 89.80 | 0.15 | 126.73 | 0.16 | 124.19 | 0.17 | 76.92 |
| Minimum | 0.11 | 1.23 | 0.10 | 0.26 | 0.13 | 0.45 | 0.13 | 12.76 |
| Maximum | 0.66 | 311.71 | 0.66 | 359.76 | 0.68 | 345.69 | 0.70 | 315.76 |

There is a strong relationship between the recorded RF data and the NDVI values obtained from each 2 degrees by 2 degrees grid. The highest $R^2$ value was observed for September, whereas the lowest value was for July (Figure 4). The strong relationship between the September RF and NDVI values could be explained by the fact that during this month, if there is adequate RF, plants can have optimal photosynthesis (high absorption of the red band of the spectrum), resulting in high NDVI values. The lowest relationship between July RF and NDVI value was unexpected and needs further research. Overall, it is convincing that we can use NDVI values to monitor drought (shortage of rainfall for monitoring agricultural drought).

**FIGURE 4**
**SCATTER PLOTS SHOWING THE CORRESPONDENCE BETWEEN THE AVERAGE NDVI AND RF FOR 1982 TO 2004**
**June (a), July (b), August (c), and September (d) are the major rainy and plant-growing months**

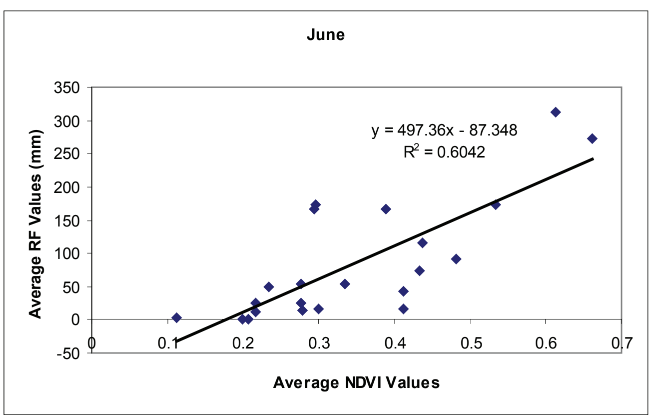


a

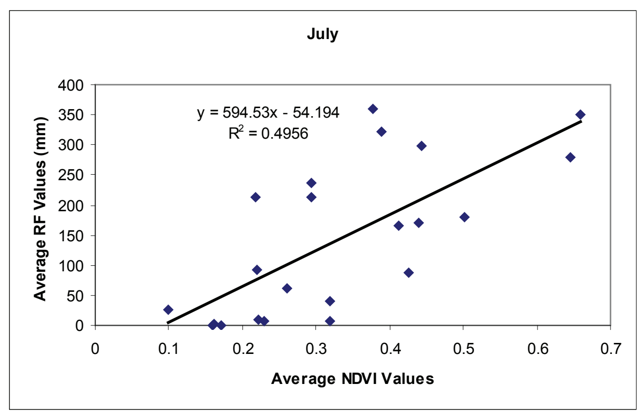


b

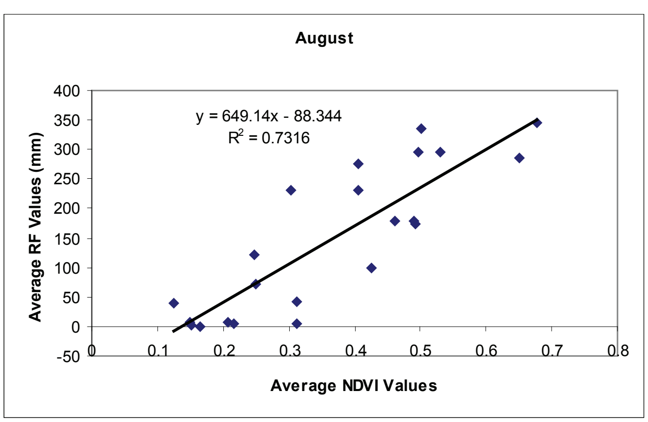


c

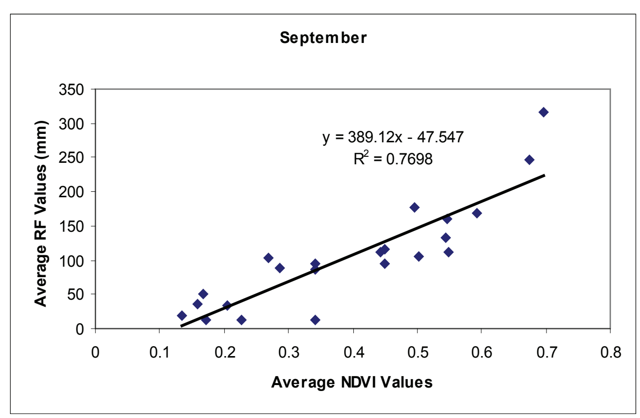


d

**NDVI and Deviation of NDVI for Spatially Locating Drought**

In this section, we present the status of drought conditions in parts of eastern African and southern Asian countries in 2009 using the NDVI parameter. Northern Sudan and southern Asian countries were purposely included in the analysis window for controlling whether the result agrees with the ground reality. These areas have no natural vegetation and the assumption is that if the result is correct, there will be no vegetation condition deviation for these areas.

This analysis was also conducted primarily with the aim of testing the applicability of MSG data for spatio-temporal drought monitoring. The preliminary results were obtained by using October 2009 MSG data and the long-term average NDVI NOAA AVHRR data. The raw MSG data were acquired from the Ethiopian Meteorological Agency in Addis Ababa. The long-term records of decadal NDVI data from NOAA were downloaded from http://earlywarning.cr.usgs.gov/adds/datathemephp and covered the first dekads of October from 1982 to 2009. Using these two datasets, the Dev_NDVI was calculated.

The actual drought condition was determined by comparing the NDVI for the first dekad of October 2009 with the long-term mean NDVI using NOAA satellite data. The data were analyzed using ILWIS 3.6 software: the 10-days images of MSG (1-10 October 2009) were imported to ILWIS raster image format using the "Multiple times in one file" option. This means that all 10 bands were stacked (maplist) together and were ready for the NDVI calculation. After importing the three-band image data to ILWIS 3.6 raster format, a script was written for calculating the Dev_NDVI.

Our results show that approximately 40% of the area exhibited negative deviation (Figures 5 and 6). Figure 6 was obtained by using the first dekad of October 2009 MSG and the 30-year long-term average NOAA AVHRR NDVI data. This indicates a prevalence of drought in 2009 in east African and southern Asian countries during the first dekad of October 2009. These results align with recorded RF in 2009 in most parts of Ethiopia; that is, the recorded rainfall amounts were below the overall average (FEWS NET, 2009).

**FIGURE 5**
**DEV_NDVI COMPARISON OF THE CHANGE IN VEGETATION**

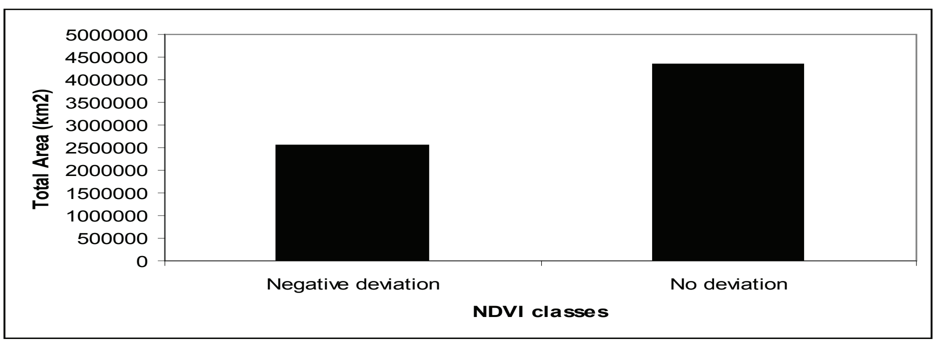


In Figure 6, the grey areas show where there is either no change or positive deviation from the long-term average. The dark grey areas show negative deviations, indicating the prevailing drought.

The analysis of the Vegetation Condition Index (VCI) also indicates the occurrence of drought in the study area (Figure 7) and shows (in percentages) the vegetation condition of the actual dekad NDVI compared to the long-term maximum and minimum of the corresponding dekad. Figure 7 was obtained by using data from the first dekad of October 2009 MSG and the 30-year long-term average NOAA AVHRR NDVI data. In principle, 50% reflects a fair vegetation condition; our geo-spatial analysis shows that approximately 37% of the total area had less than 40% VCI, indicating the occurrence of a drought. Areas with below normal vegetation cover were located in the central part of Sudan and northern and southeast Ethiopia. Only 18% of the area had optimal and above normal vegetation conditions (Figure 7); these areas are located in the central part of Sudan and the northwest corner of Ethiopia.

**FIGURE 6**
**DEV_NDVI SPATIAL DISTRIBUTION**
**1 = dark grey are areas with negative deviations indicating the prevailing drought; 2 = grey are areas where there is no change or positive deviation from the long term average. The black lines are country boundaries**

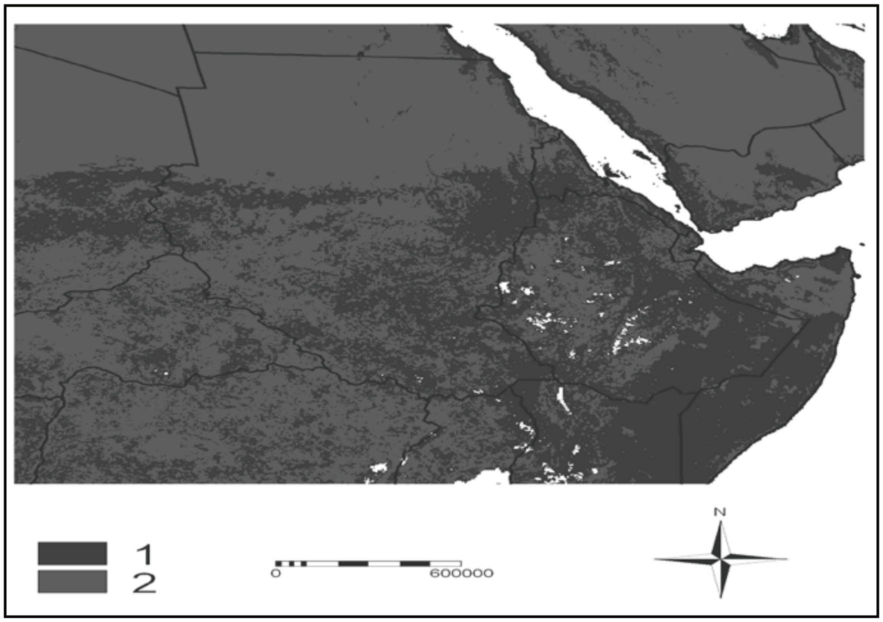


**FIGURE 7**
**VEGETATION CONDITION INDEX (VDI) MAP FOR MONITORING DROUGHT**
**Areas in white are areas where there had been no vegetation in the past and/or found to be water bodies. Country boundaries are marked in red.**

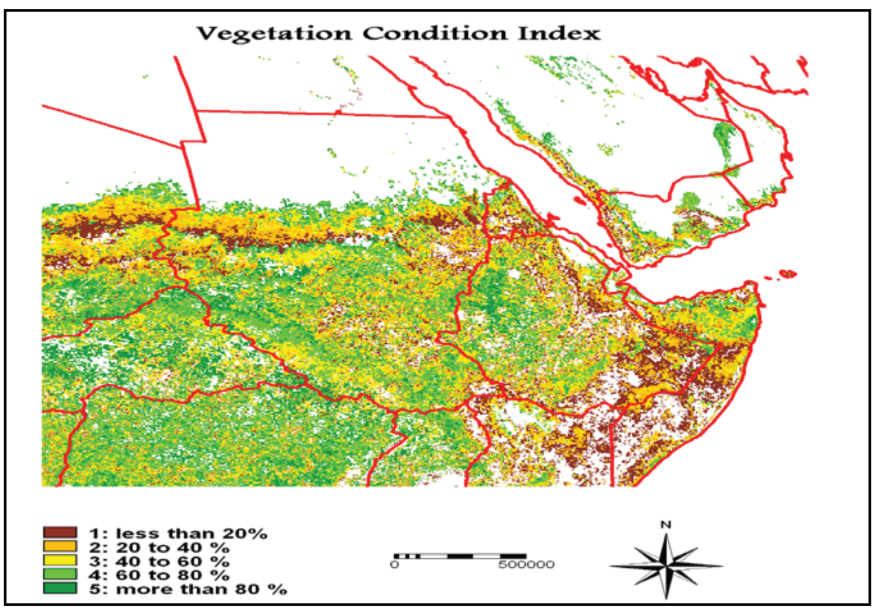

**Drought Object Extractions**

To extract drought objects, a subset image was created in the eastern part of Ethiopia (Figure 8). This area was selected because the maximum NDVI deviation value and the highest area coverage of the NDVI deviations were observed in this location. Using this subset image, the intensity of drought in the area was assessed. For this purpose, a total of 146 points were systematically generated in a point grid map of the study area.

The descriptive statistics for these 146 points are presented in Table 2. From these selected point data, about 71% of the pixels were found to have negative deviation values and about 29 pixels had positive NDVI deviations. The assumption here is that the negative NDVI deviations are revealing the prevailing drought in the area and the positive deviations are showing the healthy vegetation growth in the area during the first dekad of October 2009. The NDVI deviation values must be calibrated and must be related to the ground measurement RF records. NDVI deviation values calibrations and relating these values with actual drought intensity in the area is the future research agenda identified in this research. From the selected data sets, pixels with zero deviation value were not recorded.

The pixels were also found to have some pattern showing drought object distribution in the area. In the original image, there are ranges of negative to positive deviations. For display purposes, the negative deviations were multiplied by -1, and the original negative deviation values become positive and the positive deviations become negative. From Figure 8, it can be observed that there are some local maximum deviation values that were found to decrease gradually to local minimum values, revealing the possibility of identifying drought objects. On this figure, the red areas are pixels with maximum deviations that gradually decrease to the yellow color, and the blue colors show positive deviations of the pixels (in this case, with optimum red band use for plant photosynthesis activity or conversion of light energy into chemical energy).

The drought objects were extracted using the concepts of local maxima and local minima NDVI deviation values. The maximum deviation value recorded was -0.552. The histogram of NDVI deviation values for the whole of Ethiopia is presented on Figure 9; most of the pixels were found in the range of -0.2 to 0.1, with the highest frequency being around -0.05.

**TABLE 2**
**DESCRIPTIVE STATISTICS FOR DEV_NDVI VALUES IN THE SUBSET IMAGE**

| *No* | *Description* | Value |
|---|---|---|
| 1 | Mean | -0.077 |
| 2 | Median | -0.080 |
| 3 | Standard Deviation | 0.076 |
| 4 | Minimum | -0.282 |
| 5 | Maximum | 0.115 |

**FIGURE 8**
**3D REPRESENTATION OF NDVI DEVIATION VALUES FOR THE FIRST DEKAD OF OCTOBER 2009**
**The graph surfaces represent relatively low NDVI deviation in the blue areas and the highest deviations in the deep red areas**

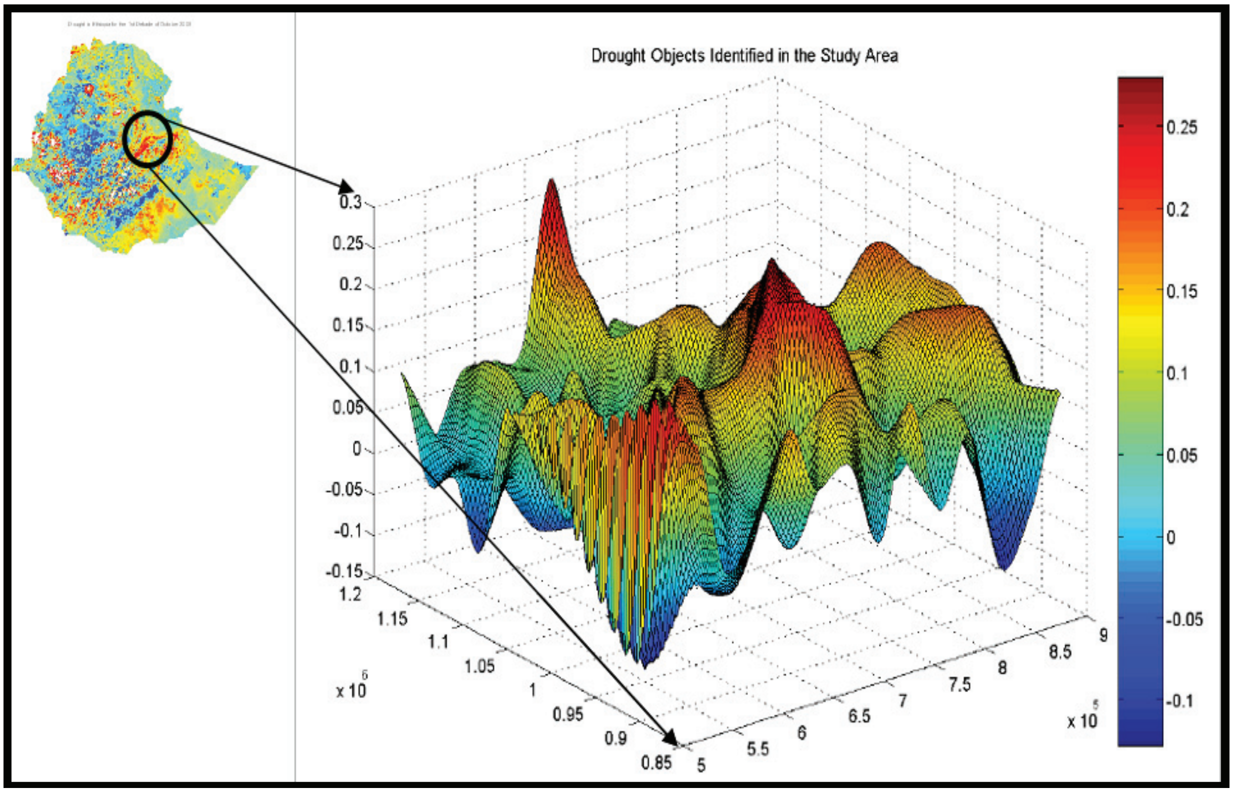


**FIGURE 9**
**HISTOGRAM FOR DEV_NDVI DISTRIBUTIONS**

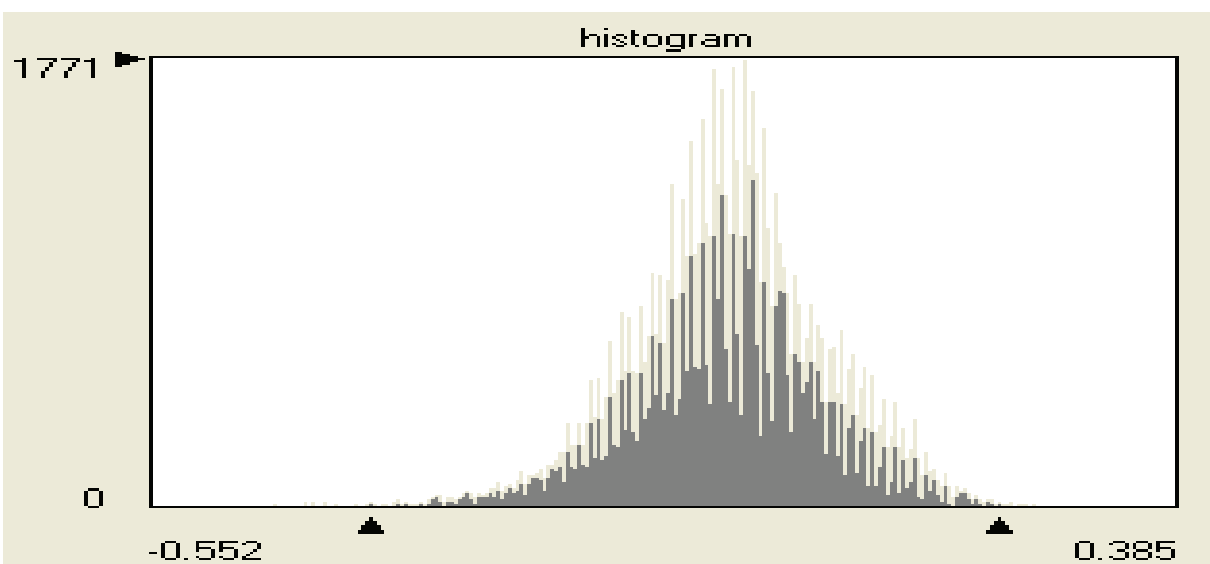

The NDVI deviation values for the whole of Ethiopia were grouped into four classes. This grouping is based on the above assumption in that negative NDVI deviations are indicative of the prevailing drought. These classes were made according to Mckee's et al. (1993) definition of drought categories of standard precipitation index (SPI). One of the future research agendas identified from this research is to calibrate and correlate the classes derived from SPI and the Dev_NDVI classes proposed from this research.

The NDVI deviation values derived from the first dekad of October 2009 were classified and presented in Table 3. Accordingly, the Dev_NDVI values range from -0.55 (severe drought) to 0.38 (above optimal). Most of the pixels were in the range of > -0.05 to <=0.1 (near normal) category, followed by > -0.2 to <= -0.05 (drought) (Figure 9). This shows that, of all the pixels assessed, drought or moderately dry has the highest share, indicating the prevalence of drought in the first dekad of October 2009 in Ethiopia. The four NDVI deviation values were classified using the Nearest Neighbor Rule classification and the map is presented in Figure 10.

Figure 10 shows that the severe drought class was observed in different parts of the country. The highest patches were observed in the north-western corner and the central part of the country. The second drought class (moderately dry) was found next to the severe drought patches in the central, northern, southern, and eastern part of Ethiopia. In this map, the white or missing values were cloud pixels and the locations were purposely excluded from drought assessment during the analysis.

The drought object extraction was done by grouping similar pixels as one object (pixels in the same drought classes and spatially neighbouring pixels were grouped to form one object). The two drought classes were extracted and their spatial distribution is presented in Figure 11. A total of 590 severe drought objects and 1243 drought objects were extracted in this analysis; the summary statistics for these drought classes are presented in Table 3.

**TABLE 3**
**NDVI DEVIATION CLASSES AND RANGE OF VALUES**

| No | **Drought classes** | **Range of Dev_NDVI values** | **Number of objects (pixels)** | **Area (ha)** |
|---|---|---|---|---|
| **1** | Sever drought (extremely dry) | <= -0.2 | 2086 | 3675594.58 |
| **2** | Drought (moderately dry) | >-0.2 AND <= -0.05 | 25937 | 45701772.11 |
| **3** | Near normal | > -0.05 AND <=0.1 | 34691 | 61126582.73 |
| **4** | Above optimum (extremely wet) | > 0.1 | 1868 | 3291472.04 |
| | Total | | 64582 | 113795421.50 |

FIGURE 10

DROUGHT CLASSES DISTRIBUTIONS OF FIRST DEKAD IN OCTOBER 2009 IN ETHIOPIA

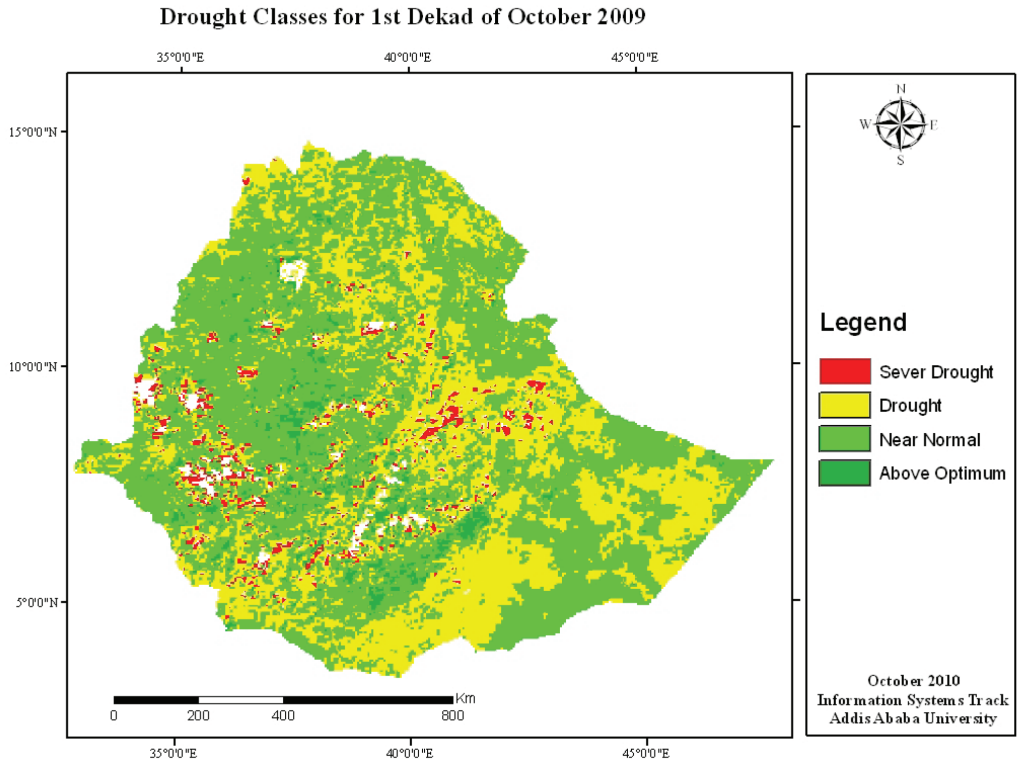


FIGURE 11

SPATIAL DISTRIBUTION OF SEVERE DROUGHT AND DROUGHT CLASSES

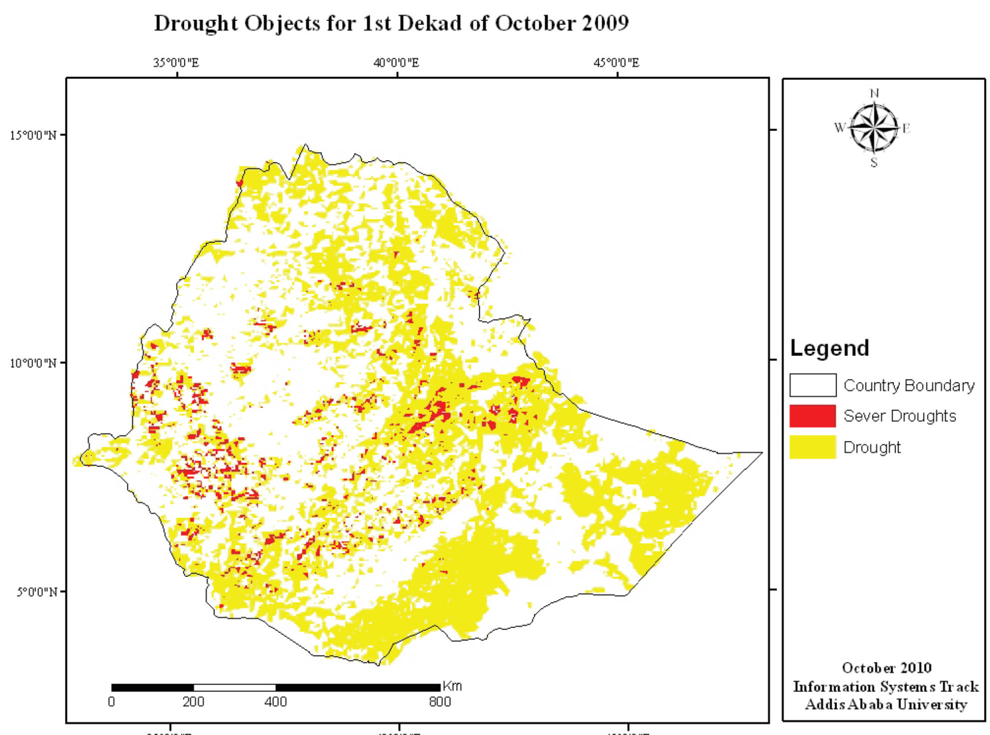

## CONCLUSIONS

In this research, the preliminary results produced promising scientific outputs for implementing satellite data for drought monitoring. This research is currently in its early stages, although there is some convincing evidence that it is possible to model and predict drought conditions using real-time MSG data. In this research, we developed a new concept and approach for extracting knowledge from satellite imageries for near real-time drought monitoring. The approach was investigated using the two known meteorological satellites, MSG and NOAA AVHRR to extract drought objects in the first dekad of October 2009 in Ethiopia. The approach was tested with the assumption that negative NDVI deviations depict the prevailing drought in the area, while the positive deviations show the healthy vegetation growth in the area. NDVI deviation value calibrations and relating these values to actual drought intensity in the area is one of the research agendas identified in this research.

The preliminary results suggest that real-time spatiotemporal MSG data can be used for drought monitoring and early warning systems in food insecure areas. In 2009, there was drought in most parts of Ethiopia and Sudan due to the RF shortage during the crop-growing season, from July to September. The results of our analysis confirm this fact.

Water and food shortage are long-term impacts of climate change and are of major concern to the world community these days. Our results could help decision makers to use advanced satellite technology for effective drought monitoring and early warning systems in various regions. Combined with proper policies, these systems can help to prevent famine and starvation in food-insecure regions. In the past, satellite technologies have been used primarily in areas of meteorological applications. In this research, the main emphasis is on mining knowledge for drought hazard assessment and saving the lives of individuals who are affected by recurring droughts. The findings of this research can assist decision makers in taking timely and appropriate actions to save lives in drought-affected areas using advanced satellite technology.

## REFERENCES


Anyamba, A., & Tucker, C. J. (2005). Analysis of Sahelian vegetation dynamics using NOAA-AVHRR NDVI data from 1981-2003. *Journal of Arid Environments, 63*(3), 596-614.

Batty, M., Dodge, M., Doyle, S., & Smith, A. ( 1998). Modelling virtual environments. In P. A. Longley, S. M. Brooks, R. McDonnell & B. MacMillan (Eds.), *Geocomputation: a Primer* (pp. 139-161.). Chichester, England: John Wiley & Sons.

Benedetti, R., & Rossini, P. (1993). On the use of NDVI profiles as a tool for agricultural statistics: The case study of wheat yield estimate and forecast in Emilia Romagna. *Remote Sensing of Environment, 45*(3), 311-326.

Benz, U. C., Hofmann, P., Willhauck, G., Lingenfelder, I., & Heynen, M. (2004). Multi-resolution, object-oriented fuzzy analysis of remote sensing data for GIS-ready information. *ISPRS Journal of Photogrammetry and Remote Sensing, 58*(3-4), 239-258.

Budd, T. (2000). *Understanding object-oriented programming with Java*. Reading, MA: Addison Wesley Longman.

Cooper, P. J. M., Dimes, J., Rao, K. P. C., Shapiro, B., Shiferaw, B., & Twomlow, S. (2008). Coping better with current climatic variability in the rain-fed farming systems of sub-Saharan Africa: An essential first step in adapting to future climate change? *Agriculture, Ecosystems & Environment, 126*(1-2), 24-35.

EMA Ethiopian Mapping Authority (Cartographer). (1988). *National Atlas of Ethiopia*.

EUMETSAT. (2005). Meteosat Second Generation In Orbit - In Use. Retrieved 18 February, 2011, from http://www.eumetsat.int/groups/cps/documents/document/pdf_br_msg02_en.pdf

Fensholt, R., Sandholt, I., Stisen, S., & Tucker, C. (2006). Analysing NDVI for the African continent using the geostationary meteosat second generation SEVIRI sensor. *Remote Sensing of Environment, 101*(2), 212-229.

FEWS.NET. (2009). United Nations' FEWS (Famine Early Warning Systems) program. Retrieved 8 December, 2009, from http://www.fews.net/Pages/default.aspx?l=en

Gregor, S. (2006). The nature of theory in information systems. *Management Information Systems Quarterly, 30*(3), 611.

Gregor, S., & Jones, D. (2007). The anatomy of a design theory. *Journal of the Association for Information Systems, 8*(5), 312-335.

Hayes, J. T., O'Rourke, P. A., Terjung, W. H., & Todhunter, P. E. (1982). YIELD: A numerical crop yield model of irrigated and rainfed agriculture. *Publications Climatology, 35*(2).

Hevner, A. R., March, S. T., Park, J., & Ram, S. (2004). Design Science in Information Systems Research. *Mis Quarterly, 28*(1), 75-105.

Holben, B. N. (1986). Characteristics of maximum-value composite images from temporal AVHRR data. *International Journal of Remote Sensing, 7*(11), 1417-1434.

Huang, B., Jiang, B., & Li, H. (2001). An integration of GIS, virtual reality and the Internet for visualization, analysis and exploration of spatial data. *International Journal of Geographical Information Science, 15*(5), 439-456.

Jain, S. K., Keshri, R., Goswami, A., Sarkar, A., & Chaudhry, A. (2009). Identification of drought-vulnerable areas using NOAA AVHRR data. *International Journal of Remote Sensing, 30*(10), 2653-2668.

Ji, L., & Peters, A. J. (2003). Assessing vegetation response to drought in the northern Great Plains using vegetation and drought indices. *Remote Sensing of Environment, 87*(1), 85-98.

Kandji, S. T., Verchot, L., & Mackensen, J. (2006). *Climate change and variability in the Sahel region: impacts and adaptation strategies in the agricultural sector*. Nairobi, Kenya: United Nations Environment Programme World Agroforestry Centre.

Kogan, F., Gitelson, A., Zakarin, E., Spivak, L., & Lebed, L. (2003). AVHRR-Based Spectral Vegetation Index for Quantitative Assessment of Vegetaton State and Productivity: Calibration and Validation. *Photogrammetric engineering and remote sensing, 69*(8), 899-906.

McKee, T. B., Doesken, N. J., & Kleist, J. (1993). *The relationship of drought frequency and duration to time scales*. Paper presented at the Eighth Conference on Applied Climatology.

Mishra, A. K., & Desai, V. R. (2005). Spatial and temporal drought analysis in the Kansabati river basin, India. *International Journal of River Basin Management, 3*(1), 31-41.

Myneni, R. B., & Asrar, G. (1994). Atmospheric effects and spectral vegetation indices. *Remote Sensing of Environment, 47*(3), 390-402.

Nicholson, S. E. (1994). Recent rainfall fluctuations in Africa and their relationship to past conditions over the continent. *The Holocene, 4*(2), 121.

NMSA National Meteorological Services Agency. (1996 ). *Assessment of drought in Ethiopia Meteorological. Research Reports Series no. 2*. Addis Ababa , Ethiopia o. Document Number).

Obasi, G. O. P. (1994). WMO's Role in the International Decade for Natural Disaster Reduction. *Bulletin of the American Meteorological Society, 75*(9), 1655-1661.

Palmer, W. C. (1965). Meteorological drought. U.S. Department of Commerce, Weather Bureau, Research Paper No. 45.

Pettorelli, N., Vik, J. O., Mysterud, A., Gaillard, J.-M., Tucker, C. J., & Stenseth, N. C. (2005). Using the satellite-derived NDVI to assess ecological responses to environmental change. *Trends in Ecology & Evolution, 20*(9), 503-510.

Prasad, A. K., Singh, R. P., Tare, V., & Kafatos, M. (2007). Use of vegetation index and meteorological parameters for the prediction of crop yield in India. *International Journal of Remote Sensing, 28*(23), 5207-5235.

Quarmby, N. A., Milnes, M., Hindle, T. L., & Silleos, N. (1993). The use of multi-temporal NDVI measurements from AVHRR data for crop yield estimation and prediction. *International Journal of Remote Sensing, 14*(2), 199 - 210.

Rulinda, C. M., Bijker, W., & Stein, A. Image mining for drought monitoring in eastern Africa using Meteosat SEVIRI data. *International Journal of Applied Earth Observation and Geoinformation, 12*(Supplement 1), S63-S68.

Simon, H. A. (1996). *The Sciences of the Artificial* (3rd ed.). Cambridge, MA: MIT Press.

Singh, R. P., Roy, S., & Kogan, F. (2003). Vegetation and temperature condition indices from NOAA AVHRR data for drought monitoring over India. *International Journal of Remote Sensing, 24*(22), 4393-4402.

Smakhtin, V. U., & Hughes, D. A. (2004). *Review, automated estimation and analyses of drought indices in South Asia. International Water Management Institute Working Paper 83* (Vol. Drought series paper 1). Colombo, Sri Lanka: International Water Management Institute (IWMI).

Smith, P. M., Kalluri, S. N. V., Prince, S. D., & DeFries, R. (1997). The NOAA/NASA Pathfinder AVHRR 8-km land data set. *PE & RS- Photogrammetric Engineering & Remote Sensing, 63*(1), 12.

Stein, A. (2008). Modern developments in image mining. *Science in China Series E: Technological Sciences, 51*(0), 13-25.

Stein, A., Hamm, N. A. S., & Ye, Q. (2009). Handling uncertainties in image mining for remote sensing studies. *International Journal of Remote Sensing, 30*(20), 5365 - 5382.

Swenson, S., & Wahr, J. (2009). Monitoring the water balance of Lake Victoria, East Africa, from space. *Journal of Hydrology, 370*(1-4), 163-176.

Tadesse, T., Brown, J. F., & Hayes, M. J. (2005). A new approach for predicting drought-related vegetation stress: Integrating satellite, climate, and biophysical data over the U.S. central plains. *ISPRS Journal of Photogrammetry and Remote Sensing, 59*(4), 244-253.

Tadesse, T., Haile, M., Senay, G., Wardlow, B. D., & Knutson, C. L. (2008). The need for integration of drought monitoring tools for proactive food security management in sub-Saharan Africa. *Natural Resources Forum, 32*(4), 265-279.

Thiruvengadachari, S., & Gopalkrishna, H. R. (1993). An integrated PC environment for assessment of drought. *International Journal of Remote Sensing, 14*(17), 3201-3208.

Thornton, P. K., Jones, P. G., Alagarswamy, G., & Andresen, J. (2009). Spatial variation of crop yield response to climate change in East Africa. *Global Environmental Change, 19*(1), 54-65.

Tucker, C. J. (1979). Red and photographic infrared linear combinations for monitoring vegetation. *Remote Sensing of Environment, 8*(2), 127-150.

Elaboration of an International Convention to Combat Desertification in Countries Experiencing Serious Drought and/or Desertification, (1994).

Unganai, L. S., & Kogan, F. N. (1998). Drought Monitoring and Corn Yield Estimation in Southern Africa from AVHRR Data. *Remote Sensing of Environment, 63*(3), 219-232.

UNISDR United Nations Secretariat of the International Strategy for Disaster Reduction. (2009). *Drought Risk Reduction Framework and Practices: Contributing to the Implementation of the Hyogo Framework for Action*. Geneva, Switzerland.

Wilhite, D. A. (2000). Drought as a Natural Hazard: Concepts and Definitions. In D. A. Wilhite (Ed.), *Drought: A Global Assessment* (pp. 89–104). London: Routledge Publishers.

Wilhite, D. A. (2005). *Drought and Water Crises: Science, Technology, and Management Issues*. Boca Raton, FL: CRC Press.

Worboys, M. F., Hearnshaw, H. M., & Maguire, D. J. (1990). Object-oriented data modelling for spatial databases. *International Journal of Geographical Information Systems, 4*(4), 369 - 383.